



ELSEVIER

Available online at www.sciencedirect.com

SCIENCE @ DIRECT®

International Journal of Engineering Science 43 (2005) 352–378

International
Journal of
Engineering
Science

www.elsevier.com/locate/ijengsci

The RNS/Prandtl equations and their link with other asymptotic descriptions: Application to the wall shear stress scaling in a constricted pipe

Pierre-Yves Lagrée^{a,*}, Sylvie Lorthois^b

^a *Lab. de Modélisation en Mécanique, UMR CNRS 7607, Boîte 162, Université Paris 6, 75252 Paris, France*

^b *Institut de Mécanique des Fluides de Toulouse, UMR CNRS 5502, 31400 Toulouse Cedex, France*

Received 15 November 2002; received in revised form 20 July 2004; accepted 25 September 2004

(Communicated by S.A. BERGER)

Abstract

In this paper, a steady laminar axisymmetrical flow in a straight constricted pipe is considered. The RNS/Prandtl equations are presented as an asymptotic limit of the Navier–Stokes equations. This set of equations is shown to include at first order several asymptotic descriptions of the full Navier–Stokes equations: the Blasius regime, interacting boundary layer theory, triple deck theory, the Poiseuille regime and double deck theory. These theories are all characterised by a constant pressure in each cross section. Thus, these equations are able to describe the transitions between flow regions that correspond to different classical asymptotic descriptions or regimes that are usually done with the full Navier–Stokes equations. One potential application is to predict the order of magnitude of the wall shear stress in a constricted pipe. This prediction will be compared with Navier–Stokes computations for a case of a severe constriction.

© 2005 Elsevier Ltd. All rights reserved.

* Corresponding author. Tel.: +33 1 44 27 25 59; fax: +33 1 44 27 52 59.

E-mail address: pyl@ccr.jussieu.fr (P.-Y. Lagrée).

URL: www.lmm.jussieu.fr/~lagree (P.-Y. Lagrée).

PACS: 47.15.-x; 47.60.+i; 83.50Ax

Keywords: Interacting boundary layer; Triple deck; Reduced Navier–Stokes

Nomenclature

Latin symbols

A	the triple deck displacement function
a, b	coefficients of a scaling law
d_1	a numerical value
f_2	boundary layer friction coefficient
f	a function describing the wall perturbation
K	a constant
H	boundary layer shape factor
p	pressure
R_0	initial radius of the pipe
Re	Reynolds number $U_0 R_0 / \nu$
r	radial variable
u, v	longitudinal and transverse velocity
WSS	wall shear stress
x	longitudinal variable
y	transverse variable from the wall

Superscripts

x^*	the longitudinal variable with dimensions
\bar{x}	the longitudinal variable in RNSP and entry IBL scales
\hat{x}	the longitudinal variable in entry short scale
\tilde{x}	the longitudinal variable in triple deck scale
\check{x}	the longitudinal variable in double deck scale
$\bar{\bar{x}}$	the longitudinal variable in IBL scale
x'	the longitudinal variable in quasi Poiseuille scale

Subscripts

U_0	incoming velocity scale
U_{Pois}	Poiseuille solution
U_{Blas}	Blasius solution
$U'_{\text{Blas}} = \frac{dU_{\text{Blas}}}{dy}$	derivative of Blasius solution
x_1, \bar{x}_1	width of the wall perturbation
LD	in the lower deck
MD	in the main deck
UD	in the upper deck

Greek symbols

α	relative size of the wall perturbation
ε	a small parameter
λ	ratio of the length of the stenosis to the radius of the pipe
A_1	used in the integral boundary layer
ν	viscosity
ρ	density
τ	non-dimensionalised wall shear stress
δ_1	boundary layer displacement thickness

1. Introduction

Estimating the order of magnitude of the wall shear stress (WSS) in a locally constricted pipe is important in numerous applications. For example, elevated wall shear stresses encountered in stenoses, i.e. local constrictions of blood vessels, play a significant role in thrombo-embolism and atherosclerotic plaques ruptures [1,29]. Of course, computing the flow in such a pipe can be achieved with great accuracy through Navier–Stokes solvers [2,3,6,25]. However, asymptotic equations provides a better understanding of the flow structure and relevant scalings, and reduces computational time. Therefore, parameters may be changed easily and their influence can be thoroughly investigated. Hence, the aim of this work is to find the appropriate scaling for the wall shear stress in a constricted pipe as a function of pertinent non-dimensional parameters using an asymptotic approach.

For that purpose, a set of equations that is sometimes referred to as reduced Navier–Stokes (RNS) equations will be our starting point. These equations, including a transverse pressure gradient, can be found either in three or two dimensions, plane or axisymmetrical, in Fletcher [7] and Tannehil et al. [31]. However, in our analysis, these equations will be used with a constant transverse pressure, i.e. the pressure is a function of x alone: $\partial_r p = 0$ or $p(x)$. In this case, the RNS equations formally correspond to the Prandtl equations, but with different boundary conditions. Therefore, they may be called RNS/Prandtl, or RNSP(x).

Following Smith [26] and other authors (e.g. [23,30]) analyses, we will show that the RNS/Prandtl equations includes many classical asymptotic descriptions for internal flows, i.e. the interactive boundary layer (IBL), the double deck and the triple deck theories, as well as Blasius and Poiseuille regimes. Thus, the RNS/Prandtl equations are able to describe the transitions between flow regions that correspond to different classical asymptotic descriptions or regimes that are usually done with the full Navier–Stokes equations.

In order to demonstrate the “universality” of the RNSP(x) equations, we will use either the least possible degeneracy principle [32], which requires the inertia–pressure–viscous force balance, or directly the results from the literature, that are classical but till have been disjoined.

The limitation of this description will also be presented. In particular, the RNSP(x) equations are not valid when $\partial_r p$ is not zero, which induces ellipticity and prevents the flow from being solved with a streamwise marching procedure. Nevertheless, this is not a very strong condition in internal flows, and will be demonstrated using the double deck and triple deck theories. In par-

particular, calculation of separated flows is possible [26,30,13]. Hence, the RNSP(x) equations may be applied in the case of a dilated pipe or aneurysm [11,2,3]. In addition, the RNSP(x) formulation can be applied to supersonic external flows (see [5]) except when there is an upstream influence from the flow downstream, which occurs in some triple deck problems [28]. A case of a hypersonic external flow has also been studied by Maslov et al. [17] by a RNS computation without obtaining branching solutions from upstream influence.

In the following, the variables with stars denote dimensional variables.

2. RNS/Prandtl equations (RNSP(x))

2.1. The RNSP(x) hypothesis

We consider a steady laminar incompressible axisymmetrical flow of a Newtonian fluid in a locally constricted axisymmetric pipe (see Fig. 1 for notations used). The radial position of the pipe is given by: $R^* = R_0^*(1 - f(x^*))$, where R_0^* is the unconstricted radius and f is the given radius perturbation. In addition, we denote by U_0^* the longitudinal velocity scale of the flow and assume that the typical length scale for transverse variations of the longitudinal velocity is R_0^* . From the Navier–Stokes equations, we obtain a longitudinal scale ($L_{RNS}^* \gg R_0^*$) from a balance between the convective term and the largest diffusive term. In other words, ($u^* \frac{\partial u^*}{\partial x^*}$) must be of the same order as $\nu \frac{\partial}{\partial r^*} (r^* \frac{\partial}{\partial r^*} u^*)$, which leads to:

$$\frac{U_0^{*2}}{L_{RNS}^*} u \frac{\partial u}{\partial x} \simeq \nu \frac{U_0^*}{R_0^{*2}} \frac{\partial}{\partial r} \left(r \frac{\partial}{\partial r} u \right), \tag{1}$$

where ν is the kinematic viscosity. Thus the longitudinal scale L_{RNS}^* equals $R_0^* Re$, where Re is the Reynolds number $Re = U_0^* R_0^* / \nu$. Finally, the pressure and transverse velocity scales are determined from a balance among the viscous term, convective term, and pressure gradient that drives the flow [32]. Of course, this is similar to the classical way to obtain the Prandtl equations although in the Prandtl case the transversal scale is deduced from an initially chosen longitudinal scale.

A similar approach will be carried out in the following sections with various transverse scales corresponding to the thickness of additional layers near the wall, and with various scales for the longitudinal velocity in these new layers. A longitudinal length scale will still be determined in order to obtain a balance among inertia, pressure, viscous forces.

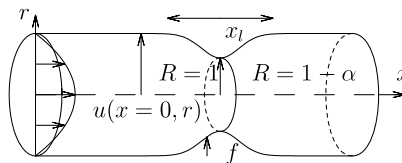


Fig. 1. Geometrical parameters of the constricted pipe. Note that the transverse scale is non-dimensionalised by the unperturbed pipe radius R_0^* . Values of x_1 and α are linked via the asymptotic scales.

2.2. The RNSP(x) formulation

As deduced from the previous section, the non-dimensional variables are given by:

$$x^* = xR_0^*Re, \quad r^* = rR_0^*, \quad u^* = U_0^*u, \quad v^* = \frac{U_0^*}{Re}v, \quad p^* = p_0^* + \rho_0U_0^{*2}p,$$

p_0^* denoting the entry pressure, and, consequently:

$$\tau^* = \mu \frac{\partial u^*}{\partial r^*} = \frac{\rho U_0^{*2}}{Re} \tau, \quad (2)$$

where τ is the WSS, μ is the dynamic viscosity and ρ the density.

With these new variables, the following partial differential system is obtained from the Navier–Stokes equations as $Re \rightarrow \infty$:

$$\frac{\partial}{\partial x}u + \frac{\partial rv}{r\partial r} = 0, \quad u \frac{\partial u}{\partial x} + v \frac{\partial u}{\partial r} = -\frac{\partial p}{\partial x} + \frac{\partial}{\partial r} \left(r \frac{\partial u}{\partial r} \right), \quad 0 = -\frac{\partial p}{\partial r}. \quad (3)$$

The associated boundary conditions are:

- the condition of axial symmetry: $\partial_r u = 0$ and $v = 0$ at $r = 0$,
- no-slip condition at the wall: $u = v = 0$ at $r = 1 - f(x)$. Of course, in order to apply the RNSP(x) set, f is of order one, but smaller than one, and the longitudinal scale has to be compatible, i.e. of scale L_{RNS}^* . In the next section, the implications of a change in the constriction height and the length will be discussed,
- the entry velocity profiles ($u(0, r)$ and $v(0, r)$) are given: flat profile or Poiseuille flow, but other profile is also possible,
- there is *no* outflow boundary condition because the system is parabolic as will be demonstrated in the linearised asymptotic descriptions. The equations are solved by marching in the stream-wise direction, even if there is flow separation.

The most important result of the computation is the non-dimensionalised WSS: $\tau = \frac{\partial u}{\partial r}(x, 0)$.

2.3. Comments

This set of equations has been already used for studying entry effects by Cebeci and Cousteix [4] and in Schlichting [24]. However, Rubin and Himansu [22] and Fletcher [7] kept a transversal pressure variation linked with the transverse velocity as follows:

$$Re^{-2} \left(u \frac{\partial}{\partial x}v + v \frac{\partial}{\partial r}v \right) = -\frac{\partial p}{\partial r} + Re^{-2} \left(\frac{\partial}{\partial r} \left(r \frac{\partial}{\partial r}v \right) - \frac{v^2}{r} \right). \quad (4)$$

They call the system (3.1), (3.2) and (4) ‘‘Reduced NS’’, but as noted by Fletcher [7], this system contains a mix of orders of magnitude, and is not coherent from an asymptotical point of view. Indeed, as Re tends toward infinity, Eq. (4) degenerates to Eq. (3), and the system (3), (4) reduces to the RNSP(x) set. Subsequently, this system is used to obtain most of the degeneracy of the full NS equations in an axisymmetrical pipe:

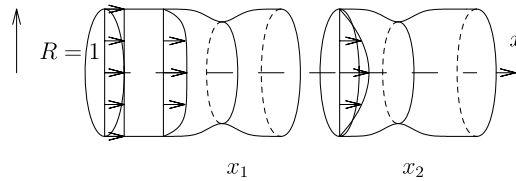


Fig. 2. Flow configurations: A constriction may be located at station x_1 where an inviscid fluid core still exists, see Section 3.2.1: IBL or Section 3.3: triple deck (Fig. 8), or at station x_2 where the Poiseuille profile has developed, see Section 3.4: double deck (Fig. 11). If the constriction is short but severe enough, the exact entrance velocity profile has no importance, see Section 3.6.1: IBL.

- In Section 3.1, a unconstricted case will be discussed (entry problem, see Fig. 3).
- In Section 3.2.1 and Section 3.3, a case of a constriction situated near the pipe entry, where the velocity profile is flat in the core flow, will be considered (see Fig. 2, left). In this case, the interacting boundary layer and the triple deck theories are valid since the core flow is inviscid and there is a thin boundary layer near the wall.
- In Section 3.4, a case of a constriction situated far from the pipe entry, where the flow is fully developed, will be considered (see Fig. 2, right). In this region, the double deck theory, also known as Smith’s theory of viscous perturbation on a Poiseuille flow in a pipe, is valid.
- Finally, in Section 3.6.1, we will show that if the constriction is short compared to R_0^*Re , the velocity profile at the entry is not important. In that case, the interacting boundary layer theory proves to be valid again: acceleration is so high that the profile flattens, recreating an inviscid core and a thin boundary layer near the wall.

In particular, the scale of the non-dimensional WSS will be determined by the location and size of the constriction. This scale will not always be of order one in the RNSP scales.

3. Link of RNSP(x) with other asymptotic descriptions

3.1. RNSP(x): from Blasius to Poiseuille

First, starting from a flat profile at the entrance ($u(0, r) = 1$ and $v(0, r) = 0$), the flow consist of two concentric layers (see Fig. 3):

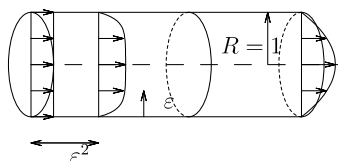


Fig. 3. Unconstricted situation: entry problem. Starting from a flat velocity profile, a Poiseuille profile is obtained at the exit, i.e. at a distance $O(1)$ in the R_0Re scale. Near the entrance, i.e. at a distance $O(\epsilon^2)$, the IBL formulation is valid: the boundary layer thickness is of order $O(\epsilon)$ in the R_0 scale.

- A first layer of length $\varepsilon^2 \ll 1$ and of transversal length 1 (except near the wall) where the velocity is uniform ($u = 1, v = 0$): the inviscid core.
- A second thin layer of the same longitudinal length $\varepsilon^2 \ll 1$, but of thickness $\varepsilon \ll 1$. In this layer, introducing $x = \varepsilon^2 \bar{x}, r = 1 - \varepsilon \bar{y}, u = \bar{u}, -v = \varepsilon^{-1} \bar{v}$ and $p = \bar{p}$, the RNSP(x) set leads to the classical Boundary Layer equations:

$$\frac{\partial \bar{u}}{\partial \bar{x}} + \frac{\partial \bar{v}}{\partial \bar{y}} = 0, \quad \left(\bar{u} \frac{\partial \bar{u}}{\partial \bar{x}} + \bar{v} \frac{\partial \bar{u}}{\partial \bar{y}} \right) = -\frac{\partial \bar{p}}{\partial \bar{x}} + \frac{\partial^2 \bar{u}}{\partial \bar{y}^2}, \quad 0 = -\frac{\partial \bar{p}}{\partial \bar{y}}, \tag{5}$$

with the following boundary conditions: $\bar{u}(\bar{x}, 0) = 0, \bar{v}(\bar{x}, 0) = 0, \bar{u}(\bar{x}, \infty) = 1, \bar{p}(\bar{x}, \infty) = 0$, corresponding to the Blasius flow regime.

Thus, if L^* denotes the current dimensional length in this second layer, i.e. $L^* = \varepsilon^2 L_{\text{RNS}}^*$, the corresponding thickness is given by εR_0^* , or

$$\sqrt{\frac{L^*}{L_{\text{RNS}}^*}} R_0^* = \frac{L^*}{\sqrt{\frac{U_0^* L^*}{\nu}}}, \tag{6}$$

the classical boundary layer thickness. Similarly, the non-dimensional WSS is the Blasius value $\bar{\tau} = 0.33 \bar{x}^{-1/2}$ [24]. Consequently, $\tau = \varepsilon^{-1} 0.33 (\varepsilon^{-2} x)^{-1/2}$, or, in dimensional form:

$$\tau^* = \left[\frac{\rho U_0^{*2}}{Re} \right] \left(0.33 \left(\frac{x^*}{R_0^*} \right)^{-1/2} \right). \tag{7}$$

Second, the Poiseuille solution is obviously a solution for the set (3) associated with the no-slip condition at the wall, with its WSS:

$$u = U_{\text{Pois}}(r) = 2(1 - r^2), \quad v = 0, \quad \tau^* = (4) \left[\frac{\rho U_0^{*2}}{Re} \right]. \tag{8}$$

Third, the system (3) allows the computation of the entry flow from Blasius to Poiseuille (see [24,4] and next Section 3.1.1).

Finally, at the entrance of the pipe, there is a small region of the same relative thickness and length $\varepsilon = Re^{-1}$ where a full Navier–Stokes problem must be solved. This degeneracy is not included in the RNSP(x). From Navier–Stokes equations, with: $x^* = \varepsilon R_0^* \hat{x}, r^* = R_0^*(1 - \varepsilon \hat{y}), u^* = U_0^* \hat{u}, v^* = U_0^* \hat{v}$ we obtain:

$$\frac{\partial \hat{u}}{\partial \hat{x}} + \frac{\partial \hat{v}}{\partial \hat{y}} = 0, \tag{9}$$

$$\hat{u} \frac{\partial \hat{u}}{\partial \hat{x}} + \hat{v} \frac{\partial \hat{u}}{\partial \hat{y}} = -\frac{\partial \hat{p}}{\partial \hat{x}} + \frac{\partial^2 \hat{u}}{\partial \hat{x}^2} + \frac{\partial^2 \hat{u}}{\partial \hat{y}^2}, \quad \hat{u} \frac{\partial \hat{v}}{\partial \hat{x}} + \hat{v} \frac{\partial \hat{v}}{\partial \hat{y}} = -\frac{\partial \hat{p}}{\partial \hat{y}} + \frac{\partial^2 \hat{v}}{\partial \hat{x}^2} + \frac{\partial^2 \hat{v}}{\partial \hat{y}^2}. \tag{10}$$

This short scale problem is the first limitation of the RNSP(x) set because $\partial \hat{p} / \partial \hat{y}$ is not zero, resulting an elliptic system. In this region, in the RNSP scales, the transversal length is of order Re^{-1} and the longitudinal velocity is of order 1. The non-dimensional WSS thus scales as Re . Finally, from Eq. (2), the physical scale of the WSS (τ^*) is given by

$$\tau^* = O(\rho U_0^{*2}). \tag{11}$$

Note that the matching between this NS short scale region and the RNS/Prandtl areas is a very difficult task. However, there is an analogy between this issue and the thermal boundary layer in a Poiseuille flow (described in Pedley [18]). First, at the entrance of the pipe, the full heat equation holds, corresponding to our full NS problem. Then, the Lévêque problem corresponds to our inviscid core/Blasius layer flow region. Finally, the Graetz problem corresponds to the Blasius/Poiseuille transition. In this problem, solutions of the full heat equations may be matched with the solution of the Lévêque problem.

3.1.1. Numerical results

The numerical solutions of the RNSP system (3) and other asymptotic descriptions in the following sections are achieved using a simple finite difference scheme in “mapped variables” [12]. The derivatives are implicit, centred in the transverse direction and marching in the streamwise direction. The core of the solution is the second order derivative with a two point boundary condition for u in Eq. (3). It is solved by the Thomas algorithm [19]. The transverse velocity is then computed by integration of Eq. (3). The idea is to guess by a Newton iteration scheme the value of the pressure at the current step so that the boundary condition for the transverse velocity is fulfilled. An alternative way to solve for the pressure gradient can be found in Felcher [7]. This code enables the computation of the boundary layer separation (reverse flow) in mild constrictions, but, if the constriction is severe, the FLARE approximation [20] must be used.

Fig. 4 displays the longitudinal evolution of the velocity at the centre of the pipe, starting from the entrance ($u(x = 0, r = 0) = 1$) and to the Poiseuille value ($u(x = \infty, r = 0) = 2$). The length of the entrance region is given by $x_e \simeq 0.214$ where $u(x_e, r = 0)/u(x = \infty, r = 0)$ equals 0.99. The asymptote obtained for small $x = 0$ values will be examined in the next section. Fig. 5 displays

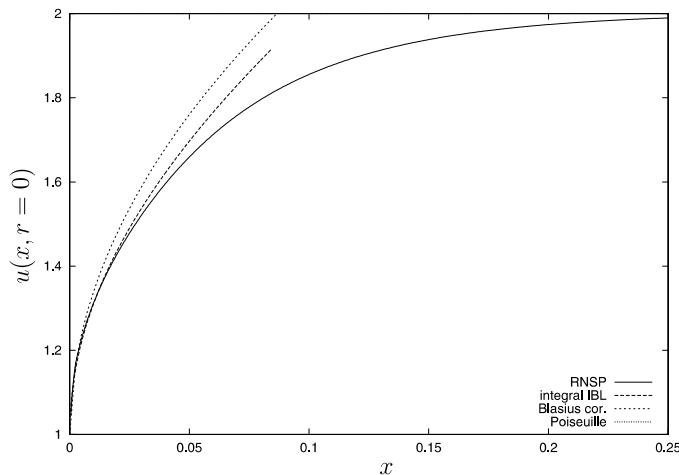


Fig. 4. Unconstricted situation: longitudinal evolution of the velocity at the centre of the pipe. RNSP: numerical solution of the RNSP equations; integral IBL: solution obtained with the integral IBL approach, rescaled in the x variable; “Blasius cor.”: first order correction ($u = 1 + 3.4x^{1/2}$) to the Blasius solution (which is $u = 1$), as obtained in Section 3.2.5. Note that the Poiseuille value is independent of x and equals 2.

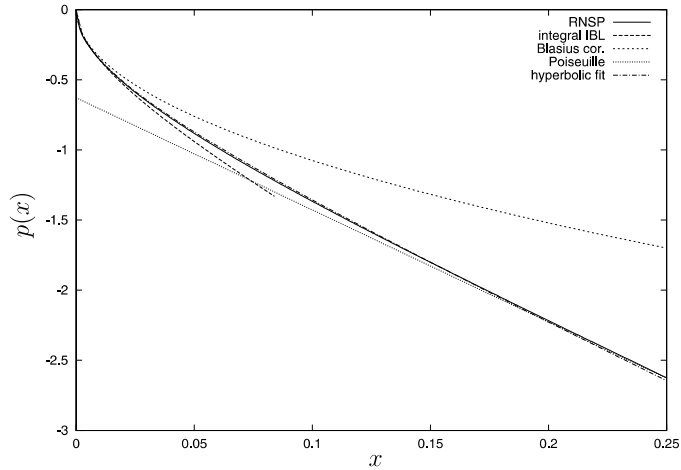


Fig. 5. Unconstricted situation: longitudinal evolution of the pressure: RNSP: numerical solution of the RNSP equations; integral IBL: solution obtained with the integral IBL approach, rescaled in the x variable; Poiseuille: $p = -0.63 - 8x$, see Section 3.1; Blasius cor.: first order correction ($-2\bar{\varepsilon}\bar{\delta}_1^{\text{Blasius}}$) to the Blasius solution (which is $p = 0$), as obtained in Section 3.2.5; hyperbolic fit: ad hoc fitting relation (Eq. (20)).

the longitudinal evolution of the pressure. For large x , the pressure asymptote is linear and of slope -8 as expected from Eqs. (5) and (8). The intercept of this asymptote corresponds to the singular pressure drop Δp_{entry} for an entry flow, i.e.: $\Delta p_{\text{entry}} = -0.63$.

3.2. RNSP(x): the link with IBL (interacting boundary layer)

3.2.1. The IBL formulation

After rescaling: $r = 1 - \varepsilon\bar{y}$, $u = \bar{u}$, $v = -\varepsilon^{-1}\bar{v}$, $x = \varepsilon^2\bar{x}$ and $p = \bar{p}$ and assuming a flat entry velocity profile, the RNSP(x) leads to the final IBL formulation as follows:

$$\frac{\partial \bar{u}}{\partial \bar{x}} + \frac{\partial \bar{v}}{\partial \bar{y}} = 0, \quad \left(\bar{u} \frac{\partial \bar{u}}{\partial \bar{x}} + \bar{v} \frac{\partial \bar{u}}{\partial \bar{y}} \right) = \bar{u}_e \frac{d\bar{u}_e}{d\bar{x}} + \frac{\partial^2 \bar{u}}{\partial \bar{y}^2}, \tag{12}$$

$$\bar{u}_e = \frac{1}{(1 - 2\varepsilon\bar{\delta}_1)}, \tag{13}$$

where $\bar{\delta}_1 = \int_0^\infty (1 - \frac{\bar{u}}{\bar{u}_e}) d\bar{y}$ and with the following boundary conditions: $\bar{u}(\bar{x}, 0) = 0$, $\bar{v}(\bar{x}, 0) = 0$ and $\bar{u}(\bar{x}, \infty) = \bar{u}_e$

3.2.2. Comments

The idea of the IBL [4,30,16] is to divide the flow into two regions: a boundary layer and an inviscid core. The Boundary Layer equations are obtained in the same way as in the preceding paragraph which led to the Blasius solution. However, in the IBL case, an outer edge velocity $\bar{u}_e = \bar{u}(\bar{x}, \infty)$, corresponding to the velocity of the inviscid core, is introduced. The outer edge velocity is not necessarily equal to 1, as in the Blasius case. These two regions are strongly interacting, so that the radius seen by the inviscid core is no longer R_0^* but $R_0^*(1 - \varepsilon\bar{\delta}_1)$. The

inviscid solution for a channel with a slow radius change is then obtained by a simple mass balance:

$$u^* = U_0^* \left[\frac{R_0^*}{R_0^*(1 - \varepsilon \bar{\delta}_1)} \right]^2,$$

where $\bar{\delta}_1$ is the boundary layer displacement thickness.

In establishing the velocity displacement relation (Eq. (13)), the key lies in the examination of the integral of the velocity over the channel cross section. This integral is decomposed using a small parameter δ_ρ such as: $1 \gg \delta_\rho \gg \varepsilon$.

$$\int_0^1 (ru) \, dr = \int_0^{1-\delta_\rho} (ru) \, dr + \int_{1-\delta_\rho}^1 (ru) \, dr + \left(\int_{1-\delta_\rho}^1 (ru_e(\bar{x})) \, dr - \int_{1-\delta_\rho}^1 (ru_e(\bar{x})) \, dr \right).$$

When δ_ρ tends to 0, the combination of the first and third terms equals $\bar{u}_e/2$, as δ_ρ is located in the inviscid core where $u = \bar{u}_e$. The second and fourth terms may be recombined using the \bar{y} boundary layer variable. As ε tends to 0 faster than δ_ρ , i.e. $\delta_\rho/\varepsilon \rightarrow \infty$, their sum is:

$$-\varepsilon \int_{\delta_\rho/\varepsilon}^0 ((1 - \varepsilon \bar{y})\bar{u}) \, d\bar{y} + \varepsilon \left(\int_{\delta_\rho/\varepsilon}^0 ((1 - \varepsilon \bar{y})\bar{u}_e(\bar{x})) \, d\bar{y} \right) \rightarrow -\varepsilon \bar{u}_e \bar{\delta}_1,$$

where $\bar{\delta}_1$ is the well known boundary-layer displacement thickness $\bar{\delta}_1 = \int_0^\infty (1 - \frac{\bar{u}}{\bar{u}_e}) \, d\bar{y}$. Finally, at order $O(\varepsilon^2)$: $\int_0^1 (ru) \, dr = \frac{\bar{u}_e}{2} - \varepsilon \bar{u}_e \bar{\delta}_1$, or:

$$\bar{u}_e(\bar{x})(1 - 2\varepsilon \bar{\delta}_1) = 1, \tag{14}$$

which may be rewritten as $\bar{u}_e(\bar{x})(1 - \varepsilon \bar{\delta}_1)^2 + O(\varepsilon^2) = 1$ to be interpreted as mass conservation.

Note that the IBL description has terms of different order of magnitude because Eq. (14) degenerates into $\bar{u}_e(x) = 1$. The interaction between the boundary layer and the inviscid core disappears and the Blasius regime is recovered. This inconsistency does not appear in the pure triple deck description.

If a constriction of height ε and of length ε^2 (i.e. $f(x) = \varepsilon \bar{f}(\bar{x})$) is introduced, the new boundary condition at $\bar{y} = 0$ is: $\bar{u}(\bar{x}, \bar{f}(\bar{x})) = 0$ and $\bar{v}(\bar{x}, \bar{f}(\bar{x})) = 0$. Using the Prandtl transform: $\bar{x} \rightarrow \bar{x}$, $\bar{y} \rightarrow \bar{y} - \bar{f}(\bar{x})$ and $\bar{\delta}_1 = \int_0^\infty (1 - \frac{\bar{u}}{\bar{u}_e}) \, d\bar{y}$, the problem reads again as (12), with a modified velocity displacement relation and an $O(\varepsilon^2)$ error:

$$\bar{u}_e(\bar{x})(1 - 2\varepsilon(\bar{\delta}_1 - \bar{f})) = 1, \tag{15}$$

with the former boundary condition at $\bar{y} = 0$ (i.e. $\bar{u}(\bar{x}, 0) = 0$ and $\bar{v}(\bar{x}, 0) = 0$).

As a conclusion, the IBL set of equations is encompassed by the RNSP(x) set at first order.

3.2.3. WSS

In dimensional form, the WSS is of order $O(\frac{\rho U_0^{*2}}{Re} \frac{\partial u}{\partial r})$, which leads to:

$$\tau^* = O\left(\varepsilon^{-1} \frac{\rho U_0^{*2}}{Re}\right). \tag{16}$$

3.2.4. The integral IBL solution

The IBL system (12) and (13) may be simplified by integrating Eq. (12) over the transverse variable \bar{y} . The following integral system is obtained (see [24,9] for the displacement thickness and the velocity for the inviscid core):

$$\frac{d}{d\bar{x}} \left(\frac{\bar{\delta}_1}{H} \right) = \bar{\delta}_1 \left(1 + \frac{2}{H} \right) \frac{d\bar{u}_e}{d\bar{x}} + \frac{f_2 H}{\bar{\delta}_1 \bar{u}_e}, \quad \bar{u}_e(\bar{x})(1 - 2\varepsilon\bar{\delta}_1) = 1, \tag{17}$$

where H is the shape factor and f_2 is the friction coefficient.

To solve this system, a closure relationship linking H and f_2 to δ_1 and \bar{u}_e is needed. By defining $A_1 = \bar{\delta}_1^2 \frac{d\bar{u}_e}{d\bar{x}}$, this closure relationship is obtained by locally approximating the velocity profile near the wall by a velocity profile of the Falkner Skan family (see [14]):

$$H = \begin{cases} H = 2.59e^{-0.37A_1} & \text{if } A_1 < 0.6 \\ H = 2.07 & \text{if } A_1 \geq 0.6 \end{cases}, \quad \text{and } f_2 = 0.94 \left(-\frac{1}{H} + \frac{4}{H^2} \right). \tag{18}$$

3.2.5. Numerical results for a straight pipe

Figs. 4–7 display the numerical solutions for the RNSP and IBL equations solved using an integral approach. For comparison, the IBL equations were solved at the RNSP scales. At these scales ($x = \varepsilon^2 \bar{x}$ and $\delta_1 = \varepsilon \bar{\delta}_1$), the integral system (17), becomes:

$$\frac{d}{dx} \left(\frac{\delta_1}{H} \right) = \delta_1 \left(1 + \frac{2}{H} \right) \frac{d\bar{u}_e}{dx} + \frac{f_2 H}{\delta_1 \bar{u}_e}, \quad \bar{u}_e(x)(1 - 2\delta_1) = 1. \tag{19}$$

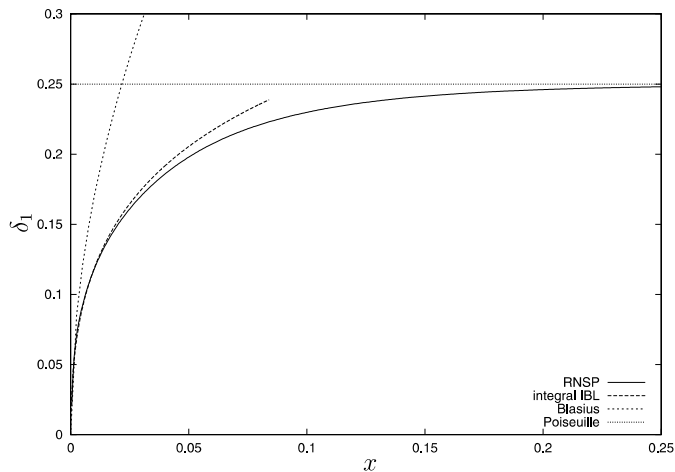


Fig. 6. Unconstricted situation: longitudinal evolution of the displacement thickness. RNSP: numerical solution of the RNSP equations; integral IBL: solution obtained with the integral IBL approach, rescaled in the x variable; Poiseuille: $\delta_1 = 1/4$; Blasius: $\delta_1 = 1.7\bar{x}^{1/2}$.

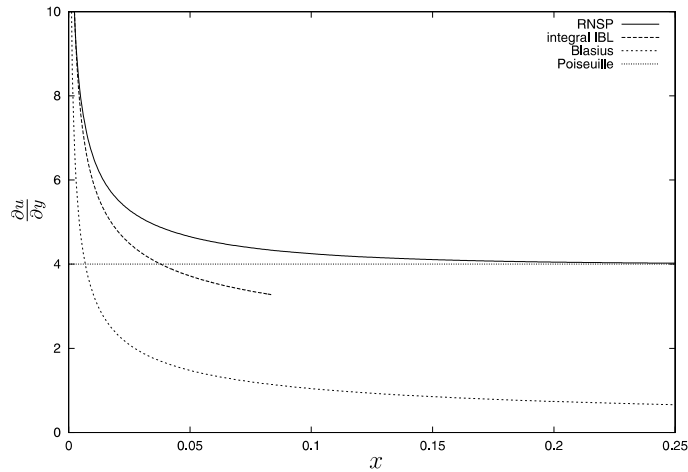


Fig. 7. Unconstricted situation: longitudinal evolution of the WSS. RNSP: numerical solution of the RNSP equations; integral IBL: solution obtained with the integral IBL approach, rescaled in the x variable; Poiseuille: $\tau = 4$; Blasius: $\tau = 0.33x^{-1/2}$.

Fig. 6 displays the evolution of the displacement thickness δ_1 obtained by the IBL integral method and its RNSP value deduced from the mass conservation relation (Eq. (14)) e.g.: $\delta_1 = 1/2 - \int_0^1 ru/u(x, 0) dr$, which is 1/4 for the Poiseuille regime. Both solutions are superimposed for small x values ($x < 0.02$). For larger x , a discrepancy appears because the IBL description does not account for the opposite wall of the pipe. Therefore, the displacement thickness monotonically increases instead of reaching a finite asymptote of value 1/4.

In addition, with the IBL approach, a first order correction to the Blasius regime near the entry in Blasius scales may be obtained. At first order in ε , the Blasius solution leads to $\bar{\delta}_1 \sim 1.7\bar{x}^{1/2}$ [24]. Thus, from Eq. (13), $\bar{u}_e \sim 1 + 2\varepsilon 1.7\bar{x}^{1/2}$, which may be rewritten in $x = \varepsilon^2\bar{x}$ scales as: $\delta_1 = \varepsilon\bar{\delta}_1 \sim 1.7x^{1/2}$ and $\bar{u}_e \sim 1 + 3.4x^{1/2}$, valid for very small x . The associated pressure is then $\bar{p} \sim 3.4x^{1/2}$. These two asymptotes are respectively plotted on Figs. 4 and 5 and labelled as ‘‘Blasius cor’’. Note that the appearance of the \sqrt{x} perturbation has been mentioned by Schlichting [24].

As displayed in Fig. 5, the longitudinal evolution of RNSP pressure behaves as the square root for small x and linearly for large x , suggesting a hyperbolic relationship. By least square regression:

$$p_{\text{hyp}} = -\frac{40}{53} \sqrt{\left(\frac{53x}{5} + 1\right)^2 - 1}. \tag{20}$$

The maximal relative error for $0 < x < .2$ between Eq. (20), as plotted in Fig. 5, and the RNSP solution is 1.2%. Note that an additional error between the RNSP and NS solutions comes from the near entry effect and may be estimated from $(\rho_0 U_0^2) Re^{-1/2}$.

Finally, Fig. 7 displays the computed evolution of the WSS that starts from the Blasius asymptote $.33x^{-1/2}$ and goes to the constant Poiseuille value for large x as predicted by the theory.

3.3. RNSP(x): the link with triple deck and IBL

3.3.1. The triple deck formulation

- *Lower deck:*

After rescaling: $r = 1 - \varepsilon^2 \tilde{y}$, $x = \varepsilon^2 + \varepsilon^5 \tilde{x}$, $u = \varepsilon \tilde{u}$, $v = -\varepsilon^{-2} \tilde{v}$ and $p = \varepsilon^2 \tilde{p}$ and assuming that $1 \gg \varepsilon^5 \gg Re^{-1}$ and a flat entry velocity profile, the RNSP(x) set leads to the final triple deck formulation as follows:

$$\frac{\partial \tilde{u}}{\partial \tilde{x}} + \frac{\partial \tilde{v}}{\partial \tilde{y}} = 0, \quad \left(\tilde{u} \frac{\partial \tilde{u}}{\partial \tilde{x}} + \tilde{v} \frac{\partial \tilde{u}}{\partial \tilde{y}} \right) = -\frac{d\tilde{p}}{d\tilde{x}} + \frac{\partial^2 \tilde{u}}{\partial \tilde{y}^2}, \quad (21)$$

with the following boundary conditions:

$$\tilde{u}(\tilde{x}, \tilde{f}(\tilde{x})) = 0, \quad \tilde{v}(\tilde{x}, \tilde{f}(\tilde{x})) = 0, \quad \tilde{u}(\tilde{x}, \tilde{y} \rightarrow \infty) \rightarrow \left(\frac{dU_{\text{Blas}}(0)}{d\tilde{y}} \right) (\tilde{y} + \tilde{A}(\tilde{x}))$$

and the pressure displacement relation

$$\tilde{p}(\tilde{x}) = 2\tilde{A}(\tilde{x}). \quad (22)$$

- *Main deck:*

The main deck scales are: $x = \varepsilon^2 + \varepsilon^5 \tilde{x}$, identical to the lower deck longitudinal scale and $r = 1 - \varepsilon \tilde{y}$, corresponding to the Blasius transversal scale. The velocity and pressure expand as:

$$u = U_{\text{Blas}} + \varepsilon u_{\text{MD}} + \dots, \quad v = -\varepsilon^{-3} v_{\text{MD}} + \dots, \quad p = \varepsilon^2 p_{\text{MD}}, \quad (23)$$

so that

$$\frac{\partial u_{\text{MD}}}{\partial \tilde{x}} + \frac{\partial v_{\text{MD}}}{\partial \tilde{y}} = 0, \quad U_{\text{Blas}} \frac{\partial u_{\text{MD}}}{\partial \tilde{x}} + v_{\text{MD}} \left(\frac{dU_{\text{Blas}}(\tilde{y})}{d\tilde{y}} \right) = 0,$$

and $\frac{\partial p_{\text{MD}}}{\partial \tilde{y}} = 0$, whose solution is:

$$u_{\text{MD}} = \tilde{A}(\tilde{x}) \left(\frac{dU_{\text{Blas}}(\tilde{y})}{d\tilde{y}} \right) \quad \text{and} \quad v_{\text{MD}} = -\frac{d\tilde{A}}{d\tilde{x}} U_{\text{Blas}}.$$

- *Upper deck:*

The upper deck scales are: $r = r$, $x = \varepsilon^2 + \varepsilon^5 \tilde{x}$ and velocity and pressure expand as:

$$u = 1 + \varepsilon^2 u_{\text{UD}} + \dots, \quad v = \varepsilon^{-3} v_{\text{UD}} + \dots, \quad p = \varepsilon^2 p_{\text{UD}} + \dots \quad (24)$$

so that $\frac{\partial u_{\text{UD}}}{\partial \tilde{x}} + \frac{\partial v_{\text{UD}}}{r \partial r} = 0$, $\frac{\partial u_{\text{UD}}}{\partial \tilde{x}} = -\frac{\partial p_{\text{UD}}}{\partial \tilde{x}}$ and $\frac{\partial p_{\text{UD}}}{\partial r} = 0$.

The boundary conditions for these two latter layers are obtained using asymptotic matching. They are presented in the following paragraphs.

Note that to be compatible with the triple deck scales, the constriction is redefined as $f = \varepsilon^2 \tilde{f}(\tilde{x})$.

3.3.2. Comments

The triple deck theory introduces a small perturbation to the Blasius regime, for which the thickness of the developed boundary layer is of order ε . The longitudinal scale of the location of the bump has thus to be of order ε^2 , as deduced from the IBL formulation.

The upper deck, the main deck and the lower deck respectively corresponding to the inviscid core, the boundary layer of transverse scale ε and a small perturbed fraction of the boundary layer close to the wall (see Fig. 8).

Briefly, the approach of Ruban and Timoshin [21] is transposed to the axisymmetrical case. A constriction of small width x_3 , such as $x = \varepsilon^2 + x_3\tilde{x}$, and of small height $\varepsilon_3\varepsilon$, such as $r = 1 - \varepsilon_3\varepsilon\tilde{y}$, is considered. It will be subsequently shown that $\varepsilon_3 = \varepsilon$ and that $x_3 = \varepsilon^5$. In the boundary layer (main deck), the longitudinal velocity is of order 1. Thus, the velocity slope $\partial u/\partial r$ is of order ε^{-1} . The velocity perturbation induced by a constriction of height $\varepsilon_3\varepsilon$ is then of order $((\varepsilon_3\varepsilon)\varepsilon^{-1}) = \varepsilon_3$. In the fraction $\varepsilon_3\varepsilon$ of the boundary layer, i.e. the lower deck, the balance of convection ($u\partial u/\partial x$)—diffusion ($\partial^2 u/\partial y^2$) leads to $x_3 = \varepsilon_3^3\varepsilon^2$. In the same way, the convection ($u\partial u/\partial x$)—pressure ($\partial p/\partial x$) balance shows that the pressure in the lower deck is of order ε_3^2 .

As the lower deck equations give a velocity perturbation of order ε_3 , the boundary layer velocity (main deck) must also be perturbed by an amount (ε_3), i.e. $u = U_{\text{Blas}} + \varepsilon_3 u_{\text{MD}}$. The perturbation of the Blasius regime is simply solved from the RNSP equations in the main deck scales, showing that this perturbation is inviscid, and that

$$u = U_{\text{Blas}} + \varepsilon_3 \tilde{A} \left(\frac{dU_{\text{Blas}}(\tilde{y})}{d\tilde{y}} \right) \quad \text{and} \quad v = -(\varepsilon^{-1} \varepsilon_3^{-2}) (d\tilde{A}/d\tilde{x}) U_{\text{Blas}}.$$

The function $-\tilde{A}$ represents the displacement of the stream lines in the boundary layer. For small \tilde{y} , the longitudinal velocity may be expanded as:

$$\left(\frac{dU_{\text{Blas}}(0)}{d\tilde{y}} \right) \tilde{y} + \varepsilon_3 \tilde{A} \left(\frac{dU_{\text{Blas}}(0)}{d\tilde{y}} \right),$$

or, in the lower deck variable ($\tilde{y} = \varepsilon_3 \tilde{y}$), as $\varepsilon_3 \frac{dU_{\text{Blas}}(0)}{d\tilde{y}} (\tilde{y} + \tilde{A})$. Hence, matching the velocity in the lower deck i.e. ($\varepsilon_3 \tilde{u}$) for large \tilde{y} with the velocity in the main deck for small \tilde{y} leads to:

$$\tilde{u} \rightarrow \left(\frac{dU_{\text{Blas}}(0)}{d\tilde{y}} \right) (\tilde{y} + \tilde{A}). \tag{25}$$

At the top of the main deck, where $U_{\text{Blas}} = 1$, the transverse velocity is $-(\varepsilon^{-1} \varepsilon_3^{-2}) d\tilde{A}/d\tilde{x}$. This velocity is transmitted to the bottom of the upper deck and, by incompressibility, the longitudinal

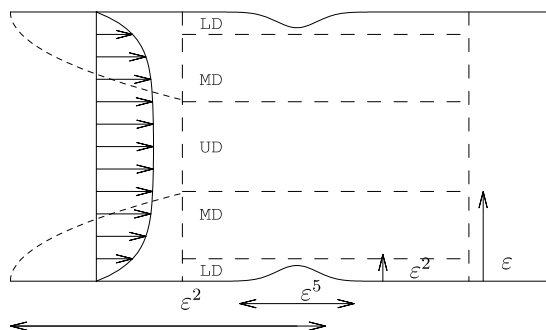


Fig. 8. Flow configuration in the triple deck case: A mild constriction, of length ε^5 and height ε^2 , is located at station ε^2 , lying in the lower deck (LD). This thin layer is included in the boundary layer of thickness ε , or main deck (MD). The upper deck (UD) is the inviscid core.

velocity perturbation u_{UD} is of order $\varepsilon_3\varepsilon$. The convection—pressure balance then shows that the pressure perturbation p_{UD} is also of order $\varepsilon_3\varepsilon$.

Finally, as the transverse pressure gradient is nul across the three layers, $\varepsilon_3\varepsilon$ is equal to the order of magnitude of the pressure in the lower deck, which is ε_3^2 (see above). Hence: $\varepsilon_3 = \varepsilon$ and $x_3 = \varepsilon^5$. In addition, the matching between the transverse velocity in the main deck for large \bar{y} and the transverse velocity in the upper deck for r close to 1 leads to $v_{UD(r \rightarrow 1)} = -(\tilde{d}\tilde{A}/\tilde{d}\tilde{x})$. Since the upper deck is irrotational, which means that u_{UD} is independent on r , the transverse velocity is $v_{UD} = -(\tilde{d}\tilde{A}/\tilde{d}\tilde{x})r/2$. Thus, by incompressibility, $\partial u_{UD}/\partial \tilde{x} = -2\tilde{d}\tilde{A}/\tilde{d}\tilde{x}$. Finally, $p_{UD} = \tilde{p} = 2\tilde{A}$.

As a conclusion, the triple deck theory is included in the RNSP(x) set.

Another interpretation of $-\tilde{A}$ is that the flux relation (Eq. (13)) is equivalent to the triple deck pressure deviation relation $\tilde{p} = 2\tilde{A}$. As done for obtaining Eq. (14), the displacement thickness is decomposed using a small parameter Y_1 such as $1 \gg Y_1 \gg \varepsilon$:

$$\begin{aligned} \bar{\delta}_1 = & \int_0^{Y_1} \left(1 - \frac{\bar{u}}{\bar{u}_e}\right) d\bar{y} + \int_{Y_1}^\infty \left(1 - \frac{\bar{u}}{\bar{u}_e}\right) d\bar{y} - \int_0^{Y_1} \left(1 - \frac{U_{Blas}}{\bar{u}_e}\right) d\bar{y} \\ & + \int_0^{Y_1} \left(1 - \frac{U_{Blas}}{\bar{u}_e}\right) d\bar{y}. \end{aligned} \tag{26}$$

In this case, $\bar{u}_e = U_{Blas}(\infty) = 1$. The combination of the first and third terms is evaluated in the lower deck where $\bar{u} = \varepsilon\tilde{u}$ and $\bar{y} = \varepsilon\tilde{y}$ as:

$$\int_0^{Y_1/\varepsilon} (1 - \varepsilon\tilde{u})\varepsilon d\tilde{y} + \int_0^{Y_1/\varepsilon} \left(1 - \varepsilon\tilde{y} \left(\frac{dU_{Blas}(0)}{d\tilde{y}}\right)\right)\varepsilon d\tilde{y}, \tag{27}$$

which is of order ε^2 . The combination of the second and fourth terms is calculated when Y_1 approaches 0, i.e. in the main deck where

$$u = U_{Blas} + \varepsilon A \left(\frac{dU_{Blas}(\bar{y})}{d\bar{y}}\right),$$

so that the Blasius displacement thickness is reobtained plus a small term

$$-\varepsilon \int_0^\infty A \left(\frac{dU_{Blas}(\bar{y})}{d\bar{y}}\right) d\bar{y}$$

which equals $-\varepsilon A$. Therefore we obtain from Eq. (26):

$$\bar{\delta}_1 = \int_0^\infty (1 - U_{Blas}) d\bar{y} - \varepsilon A + O(\varepsilon^2) = \bar{\delta}_{1,Blas} - \varepsilon A + O(\varepsilon^2). \tag{28}$$

Linearisation of Eq. (13) with this value of $\bar{\delta}_1$ gives a velocity perturbation of $-\tilde{2}\tilde{A}$, opposite to the pressure perturbation. Thus, the pressure deviation relation is $\tilde{p} = 2\tilde{A}$.

Note that the linearised solution of (21) may be obtained (see [8]) and that, as no eigen function is found, the problem is parabolic. However, if ε is decreased to $Re^{-1/5}$, $x_3 = Re^{-1}$ and the constriction width equals the pipe diameter. Thus the RNSP(x) equations no longer hold because the upper deck fills up the entire pipe cross section and there is a transverse pressure gradient (see [27]).

If the constriction is short, the influence of the opposite wall disappears. The triple deck with the pressure deviation law [28]:

$$p = \frac{1}{\pi} \int_{-\infty}^{\infty} \frac{A'}{x - \xi} d\xi,$$

is valid. This problem is not included in the RNSP(x) equations because the transverse pressure gradient has not been taken into account.

In conclusion, the triple deck equations are equivalent to the RNSP(x) equations (at first order) for all the relative scales:

$$Re^{-1/5} \ll \varepsilon \ll 1.$$

3.3.3. WSS

The WSS τ^* is $O([\varepsilon^{-1} \frac{\rho U_0^2}{Re}])$, the same as the IBL scale.

3.3.4. Incipient separation: comparison with IBL

The IBL equations (12), and (15), and the triple deck equations (21) and (22) were solved with the “semi inverse” method [16]. This is an iterative process, iteration is done on δ_1 or \tilde{A} : the “Prandtl” part (12.1) and (12.2) or (21) is solved for the pressure with a finite difference scheme with δ_1 or \tilde{A} imposed, then pressure displacement is solved for the pressure (15) or (22), the new value of δ_1 or \tilde{A} is updated from the difference of pressures until convergence. The constriction shape is $\bar{f} = \alpha \exp(-2(K(\bar{x} - 1)/\bar{x}_1))^2$, with $K = \sqrt{\ln(2)}$ for the IBL and the integral IBL problems. The constriction f is proportional to $\exp(-2(K(\tilde{x} - 2)))^2$, with $K = \sqrt{\ln(2)}$ for the triple deck problem. Fig. 9 displays the WSS at incipient separation, i.e. flow configuration where the WSS equals zero only at one point (the shear stresses are rescaled by the flat case). All the methods (RNSP, IBL, integral IBL and triple deck) show a good agreement, even if the slope discontinuity

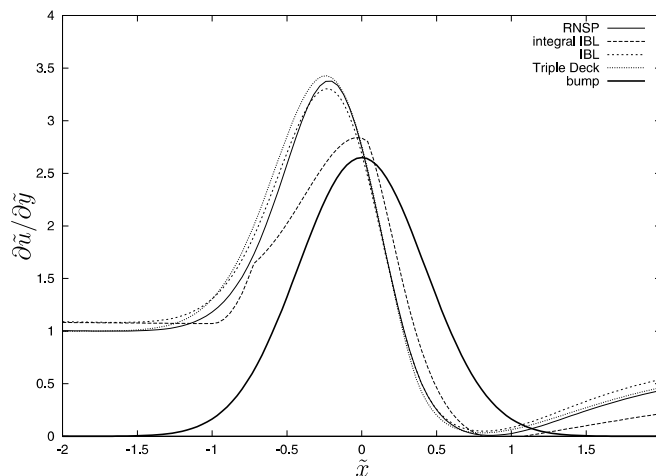


Fig. 9. Longitudinal evolution of the WSS near the incipient separation case RNSP, integral IBL, full IBL resolution (in RNSP variables, the bump is located in $x = 0.02$, and its width is 0.00125), and triple deck resolution. All the curves are rescaled in triple deck scales.

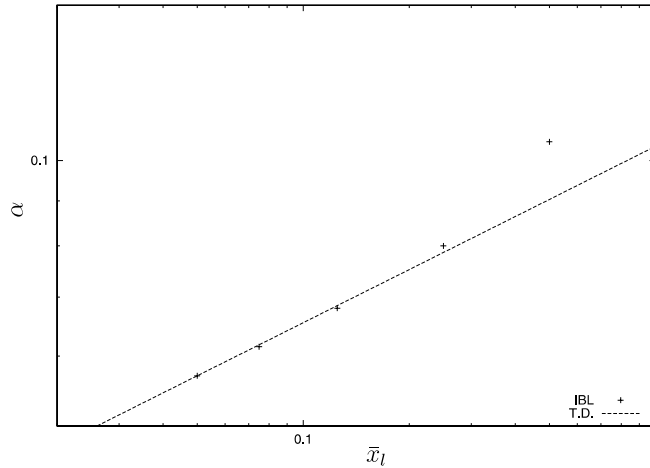


Fig. 10. Incipient separation: comparison between triple deck and IBL: value of α that promotes the incipient separation versus the longitudinal width of the constriction \bar{x}_1 computed by the full IBL equations. The line of slope 1/5 (i.e. $\alpha \simeq \bar{x}_1^{1/5}$) is the triple deck prediction.

on the integral IBL curve, corresponding to the value $A_1 = 0.6$ where the derivative of H is discontinuous (Eq. (18)) is visible. For a given boundary layer thickness ε^2 , the value of α that promotes the incipient separation at different constriction widths \bar{x}_1 was numerically sought using the IBL equations. From the triple deck theory, α/ε is the relative perturbation in the lower deck, and it behaves like $\bar{x}_1^{1/5}$. As shown on Fig. 10 for $\varepsilon^2 = 10^{-3}$, this prediction is valid up to $\bar{x}_1 = 0.3$.

3.4. RNSP(x): the link with double deck equations

3.4.1. The double deck formulation

- *Lower deck:*

After rescaling: $r = 1 - \varepsilon 4^{-1/3} \check{y}$, $x = 1 + \varepsilon^3 \check{x}$, $u = 4^{2/3} \varepsilon \check{u}$, $v = -4^{1/3} \varepsilon^{-1} \check{v}$ and $p = 4^{8/3} \varepsilon^2 \check{p}$ and assuming a Poiseuille entry velocity profile, the RNSP(x) set leads to the final double deck formulation as follows:

$$\frac{\partial \check{u}}{\partial \check{x}} + \frac{\partial \check{v}}{\partial \check{y}} = 0, \quad \left(\check{u} \frac{\partial \check{u}}{\partial \check{x}} + \check{v} \frac{\partial \check{u}}{\partial \check{y}} \right) = -\frac{d\check{p}}{d\check{x}} + \frac{\partial^2 \check{u}}{\partial \check{y}^2}, \quad (29)$$

with the following boundary conditions: $\check{u}(\check{x}, \check{f}(\check{x})) = 0$, $\check{v}(\check{x}, \check{f}(\check{x})) = 0$ and $\check{u}(\check{x}, \check{y} \rightarrow \infty) \rightarrow \check{y}$. Note that the Prandtl transform leads to $\check{u}(\check{x}, 0) = 0$, $\check{u}(\check{x}, \check{y} \rightarrow \infty) \rightarrow \check{y} - \check{f}(\check{x})$.

- *Main deck:*

The main deck scales are $x = 1 + \varepsilon^3 \check{x}$, identical to the lower deck longitudinal scale, and $r = 1 - y$, corresponding to the Poiseuille transverse scale. Velocity and pressure expand as:

$$u = U_{\text{Pois}} + \dots, \quad v = 0 + \dots \quad p = 0 + \dots$$

To be compatible with the double deck scales, the constriction is defined by $f = 4^{-1/3} \varepsilon \check{f}(\check{x})$.

3.4.2. Comments

The double deck theory introduces a small perturbation to the Poiseuille regime. In this theory, the flow is divided into two regions (see Fig. 11): the fully viscous region (main deck) and a boundary layer of transverse scale $\varepsilon 4^{-1/3}$. The equations are directly obtained from Smith [26] or transposed from Saintlos and Mauss [23] to the axisymmetrical case. The matching condition $\check{u}(\check{x}, \check{y} \rightarrow \infty) \rightarrow \check{y}$ comes from the fact that the Poiseuille velocity in the core flow (main deck) is of value $U_{\text{Pois}} = 2(1 - r^2)$ but is $4^{2/3}\varepsilon\check{y}$ near the wall as ε tends to 0. This velocity must match the velocity at the outer edge of the lower deck (i.e. $4^{2/3}\varepsilon\check{u}(\check{x}, \infty)$). Note that the full double deck theory is directly derived from the NS description. In this description, the perturbations in the main deck have to be sought as:

$$u = 2(1 - r^2) + \varepsilon u_{\text{MD}} + \dots; \quad v = \varepsilon^{-2} v_{\text{MD}} + \dots; \quad p = \varepsilon^2 p_{\text{MD}}. \tag{30}$$

Solving these perturbations either from the full NS or from the RNSP(x) equations leads to:

$$\frac{\partial u_{\text{MD}}}{\partial \check{x}} + \frac{\partial v_{\text{MD}}}{\partial \check{y}} = 0; \quad \left(U_{\text{Pois}} \frac{\partial u_{\text{MD}}}{\partial \check{x}} + v_{\text{MD}} \frac{dU_{\text{Pois}}}{d\check{y}} \right) = 0. \tag{31}$$

However the development obtained for p_{MD} from the full NS description is:

$$U_{\text{Pois}} \frac{\partial v_{\text{MD}}}{\partial \check{x}} = -(\varepsilon^7) Re^2 \frac{\partial p_{\text{MD}}}{\partial \check{y}}. \tag{32}$$

- First, the double deck theory requires that ε is smaller than one. If $\varepsilon \gg Re^{-2/7}$, Eq. (32) leads to $\frac{\partial p_{\text{MD}}}{\partial \check{y}} = 0$, which is consistent with the RNSP equations. In other words, if $\varepsilon \gg Re^{-2/7}$ (or $Re\varepsilon^3 \gg Re^{1/7}$), the RNSP(x) equations are equivalent to the double deck equations and the transverse pressure gradient is not relevant.
- Second, when $\varepsilon = Re^{-2/7}$, corresponding to real constriction length $R_0^* Re^{1/7}$ and height $R_0^* Re^{-2/7}$, the RNSP(x) is no longer valid. However, it may be shown that the pressure drop is linked to the second derivative of the displacement function \check{A} . In particular, in the symmetrical case, it may be shown [26] that $v_{\text{MD}} = 0$ (so $\check{A} = 0$). This is why the RNSP(x) set remains valid for symmetric case even if $\varepsilon = Re^{-2/7}$.

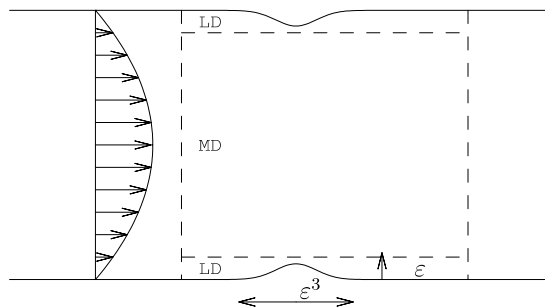


Fig. 11. Flow configuration in the double deck case: A mild constriction is located at a station where a Poiseuille flow has developed. Its length is ε^3 and its height is ε , such as it lies in the lower deck (LD). The core flow is the main deck (MD).

- Third, if $\varepsilon \ll Re^{-2/7}$, from Eq. (32), the equation at first order of ε is $\frac{\partial v_{MD}}{\partial \tilde{x}} = 0$ and its solution $v_{MD} = 0$. Thus, perturbations appear at higher orders. Consequently, $\frac{\partial p_{MD}}{\partial y} = 0$. The value $\varepsilon = Re^{-1/3}$, at which the physical longitudinal scale is R_0^* , is included in this scenario.
- Finally at short scale when the variations of x^* and y^* are of same order, a full NS problem is encountered. This corresponds to $\varepsilon^3 Re R_0^* = \varepsilon R_0^*$. Thus, for the double deck equations to hold, ε must be greater than $Re^{-1/2}$.

In conclusion, the double deck equations are equivalent to the RNSP(x) equations (at first order) for all the relative scales:

$$Re^{-1/2} \ll \varepsilon \ll 1.$$

3.4.3. WSS

The skin friction τ^* is $O(4(\rho U_0^{*2}/Re))$ for a constriction of physical length $R_0^* < \varepsilon^3 Re R_0^* \ll R_0^* Re^{1/7}$ and of height εR_0^* .

3.4.4. Incipient separation: comparison with RNSP

Starting from a Poiseuille flow, a constriction $R(x) = 1 - \alpha \exp(-(2K(x - x_c)/x_1)^2)$, with $\exp(-K^2) = 0.5$, was introduced, which corresponds to $f(\tilde{x}) = \alpha_{DD} \exp(-(2K\tilde{x})^2)$ in the double deck description. The equation is the same as in the triple deck case, but the scales are different.

Fig. 12 displays the WSS near incipient separation, showing a good agreement between the RNSP and the double deck solutions in the case of a small constriction.

Then, the value of α that promotes incipient separation for increasing constriction widths x_1 was numerically sought using the RNSP equations. Fig. 13 displays the value of α , denoted α_{IS} , as a function of x_1 . As expected from the double deck theory, which implies that:

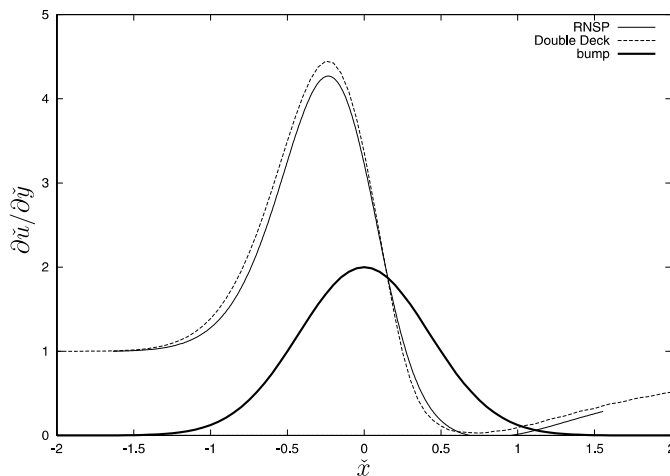


Fig. 12. Longitudinal evolution of the WSS near the incipient separation case for $x_1 = 0.0125$. DD: double deck resolution; RNSP: RNSP resolution rescaled in double deck scales.

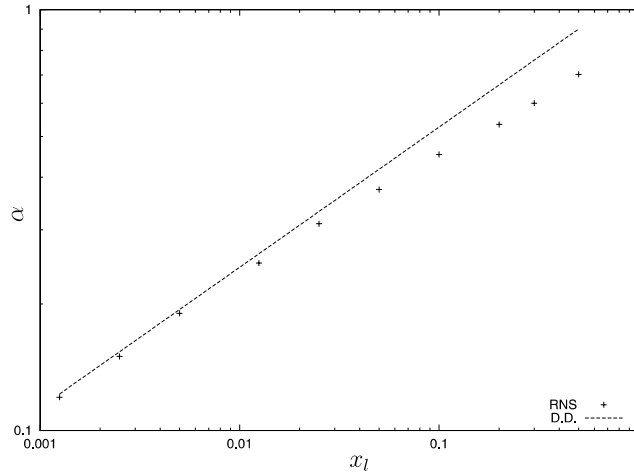


Fig. 13. Incipient separation: comparison between double deck and RNSP: value of α which promotes the incipient separation versus the longitudinal width of the constriction x_1 computed by the RNSP approach. The line of slope 1/3 (i.e. $\alpha \simeq x_1^{1/3}$) is the double deck prediction.

$$\alpha_{IS} = \alpha_{DD,IS}(4^{-1/3})(x_1)^{1/3}, \tag{33}$$

where $\alpha_{DD,IS}$ is the unique double deck incipient separation angle, α_{IS} behaves as $x_1^{1/3}$. Numerical resolution of the double deck equations led to $\alpha_{DD,IS} \simeq 2.0$. The curve $2 \cdot (4^{-1/3})(x_1)^{1/3}$ is referred as “DD” on Fig. 13.

3.4.5. Maximum value of WSS for a given constriction

Finally, increasing the constriction angle in the double deck scales, with $6 > \alpha_{DD} > 0$, the maximum value of the WSS is fitted as:

$$1.11 + 0.984\alpha_{DD} + 0.28\alpha_{DD}^2. \tag{34}$$

Expressing α_{DD} as a function of x_1 and α in Eq. (34) and multiplying by $4(\rho U_0^2/Re)$, the asymptotic maximum WSS obtained in the case of a small constriction is thus given by:

$$4(\rho U_0^2/Re) \left(1.11 + 0.984 \frac{4^{1/3}\alpha}{x_1^{1/3}} + 0.28 \frac{4^{1/3}\alpha^2}{x_1^{1/3}} \right). \tag{35}$$

3.5. RNSP(x): the link with quasi Poiseuille flow

After rescaling $x = Xx'$, with $X \gg 1$, $r = r'$, $v = X^{-1}v'$ and $p = Xp'$, the RNSP(x) set leads at first order in X^{-1} to the classical quasi Poiseuille flow: each velocity profile is a Poiseuille one. The well known relation for the WSS is obtained (for extremely large constrictions i.e. larger than R_0^*Re in physical scales):

$$\tau^* = 4(\rho U_0^{*2} Re^{-1}) \left(\frac{R_0^*}{R^*(x)} \right)^3. \tag{36}$$

3.6. RNSP(x): the link with another IBL case

3.6.1. Final formulation

After rescaling $r = R(\bar{x}) - (\lambda/Re)^{-1/2}\bar{y}$, $u = \bar{u}$, $v = -(\lambda/Re)^{1/2}\bar{v}$, $x - x_b = (\lambda/Re)\bar{x}$ and $p = \bar{p}$, where x_b is the position of the constriction throat and λR_0^* the width of the throat, the RNSP(x) set leads to the final IBL (Interacting Boundary Layer) formulation as follows:

$$\frac{\partial \bar{u}}{\partial \bar{x}} + \frac{\partial \bar{v}}{\partial \bar{y}} = 0, \quad \left(u \frac{\partial \bar{u}}{\partial \bar{x}} + v \frac{\partial \bar{u}}{\partial \bar{y}} \right) = u_e \frac{d\bar{u}_e}{d\bar{x}} + \frac{\partial^2 \bar{u}}{\partial \bar{y}^2}, \quad (37)$$

$$\bar{u}_e = \frac{1}{(R^2 - 2(\lambda/Re)^{-1/2}\bar{\delta}_1)}, \quad (38)$$

where $\bar{\delta}_1 = \int_0^\infty (1 - \frac{\bar{u}}{\bar{u}_e}) d\bar{y}$, and with the following boundary conditions: $\bar{u}(\bar{x}, 0) = 0$, $\bar{v}(\bar{x}, 0) = 0$ and $\bar{u}(\bar{x}, \infty) = \bar{u}_e$.

3.6.2. Comments

The constriction throat is located at station x_b , and is of relative length in RNSP (λ/Re).

The equations are almost identical to Eqs. (12) and (13) in the IBL section (Section 3.2.1) except the flux conservation relation (Eq. (38)). In the previous IBL section, the transition from a flat profile to a Poiseuille profile has been discussed. In a severe constriction the opposite occurs: the Poiseuille profile becomes a flat profile associated with an inviscid core. The IBL formulation again applies, but new scales have to be introduced (see [14,15]). This will be numerically verified in the following section where the RNSP(x) solution shows a flat profile at the throat for any given entry profile.

3.6.3. WSS

Using this IBL point of view, an heuristical evaluation of the WSS may be found. If the relative aperture of the constriction $1 - \alpha$ is small, i.e. $(1 - \alpha) \ll 1$, the order of magnitude of the velocity obtained by flux conservation increases from 1 at the pipe inlet to $1/(1 - \alpha)^2$ at the constriction throat. If λR_0^* represents the constriction length, R_0^* the common scale in x and y and Re the Reynolds number, the transverse velocity scale in the boundary layer is then $(1 - \alpha)\lambda^{1/2} Re^{-1/2}$.

The displacement thickness is then

$$\delta_1 = d_1(1 - \alpha)\lambda^{1/2}Re^{-1/2}, \quad (39)$$

where d_1 is an O(1) numerical value. The first correction to the velocity is from the displacement thickness δ_1 , whose effect is to increase the constriction felt by the inviscid core. The velocity is thus slightly greater than $(1 - \alpha)^{-2}$ and may be evaluated by $(1 - \alpha - \delta_1)^{-2}$. As $\lambda^{1/2}Re^{-1/2} \ll 1$, Eq. (13) leads to the following approximation for the velocity:

$$u = (1 + 2d_1((Re/\lambda)^{-1/2}))(1 - \alpha)^{-2}. \quad (40)$$

The displacement thickness corrected by this extra acceleration is:

$$\delta_1 = d_1(1 - \alpha - d_1(1 - \alpha)\lambda^{1/2}Re^{-1/2})\lambda^{1/2}Re^{-1/2}. \quad (41)$$

Finally, the WSS at the constriction throat may be approximated as the ratio of Eqs. (40) and (41) divided by 4, which is the Poiseuille WSS:

$$\text{WSS} = \left(\mu \frac{\partial u^*}{\partial y^*} \right) / \left(\left(\mu \frac{4U_0^*}{R^*} \right) \right) \sim 0.22 \frac{((Re/\lambda)^{1/2} + 3)}{(1 - \alpha)^3}. \tag{42}$$

The numerical coefficient 0.22 is based on the assumption that flow acceleration at the constriction throat corresponds to the value of a convergent channel (see [9,24] and Section 3.2.4 for the definition of H and f_2), for which $Hf_2/4=0.22$. In addition, it is assumed that $d_1 \sim 1$. Note that details on the integral method and closure relationships may be found in Lorthois and Lagrée [14]. The constriction recreates an interacting boundary layer flow. Therefore, the relevant Reynolds number is no longer Re but $Re\lambda$ and $(Re\lambda)^{1/2}$ is the inverse of the relative boundary layer thickness.

3.6.4. Comparison with NS and RNSP(x)

- *Comparison with NS:*

Siegel et al. [25] have numerically solved the NS equations in a constricted pipe. Based on their results, they postulated an ad hoc dependence for the maximal WSS as:

$$\text{WSS}_{\text{max,Sieg}} = aRe^{1/2} + b, \tag{43}$$

where coefficients a and b were dependent on the constriction geometrical parameters α and λ . On the contrary, the IBL approach led to the universal scaling law Eq. (42). This heuristical scaling law has first been numerically tested by solving the IBL system using an integral formulation. The regression analysis of the numerical results for various shapes led to:

$$\text{WSS}_{\text{max}} = \left(\mu \frac{\partial u^*}{\partial y^*} \right) / \left(\left(\mu \frac{4U_0}{R} \right) \right) \sim 0.231 \left(\frac{(Re/\lambda)^{1/2}}{(1 - \alpha)^{3.311}} + \frac{3.11}{(1 - \alpha)^{2.982}} \right). \tag{44}$$

Note that the coefficients are very close to the theoretical ones (see Eq. (42)), and they show very good agreement with the numerical values derived from Siegel et al. [25] (see Fig. 14).

- *Comparison with RNSP(x):*

The set of RNSP(x) equations has been solved by the marching finite-differences scheme. Fig. 15 displays the evolution of the velocity profile along the convergent part of a 70% constriction, for two different imposed entry profiles: a flat profile (fully potential entry) and a Poiseuille profile (fully viscous entry). As expected, when the entry flow is fully viscous, strong flow acceleration causes the velocity profile to flatten. At the constriction throat, the flow is thus independent of the entry velocity profile. In particular, the maximal WSS is in good agreement (3% discrepancy) with the maximal WSS obtained by the IBL scaling law (Eq. (44)) (see Fig. 16). In conclusion, the described set of RNS equations is “fully interactive” without any matching step and well suited for studying flow fields in constrictions.

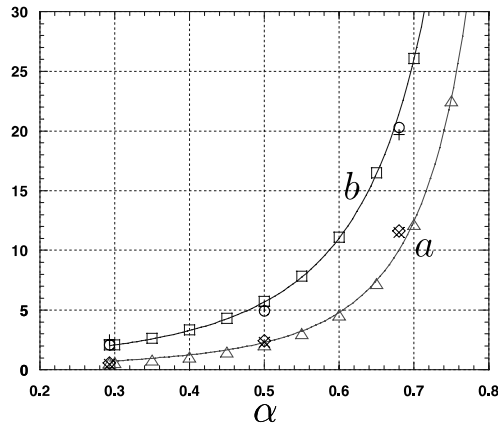


Fig. 14. Coefficient a and b for the maximum WSS (see Eq. (43)). \diamond : coefficient a derived from Siegel for $\lambda = 3$; \times : coefficient a derived from Siegel for $\lambda = 6$; \circ : coefficient b derived from Siegel for $\lambda = 3$; $+$: coefficient b derived from Siegel for $\lambda = 6$. Coefficients a (\triangle) and b (\square) obtained using the IBL integral method; solid lines: Coefficients a and b from Eq. (44).

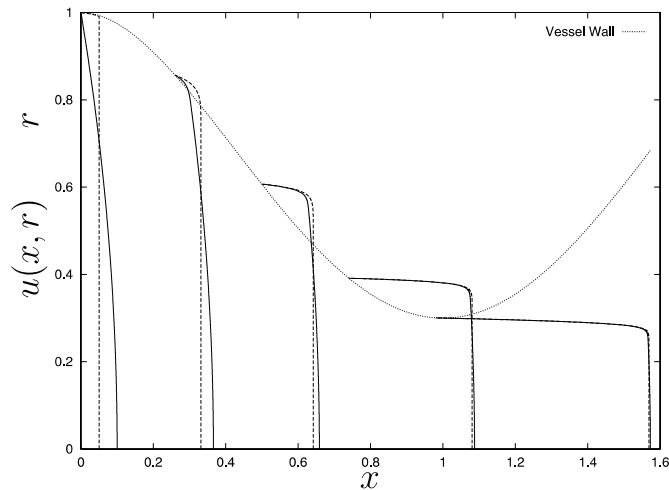


Fig. 15. Evolution of the velocity profile along the convergent part of a 70% stenosis computed using the RNSP approach, with $Re = 500$; solid line: Poiseuille entry profile; broken line: flat entry profile.

Siegel et al. [25] and Huang et al. [10] have numerically solved Navier–Stokes equations for $100 < Re < 1000$. The results obtained are consistent with our method. Furthermore, the bidimensional counterpart of this RNSP and IBL theories has been settled in Lagrée et al. [13]. Some comparisons have been done with a NS solver focusing on the pressure $p(x)$ and on the reverse flow. It has been observed that for Re from 100 to 1000, IBL, RNSP, and NS give very similar results.

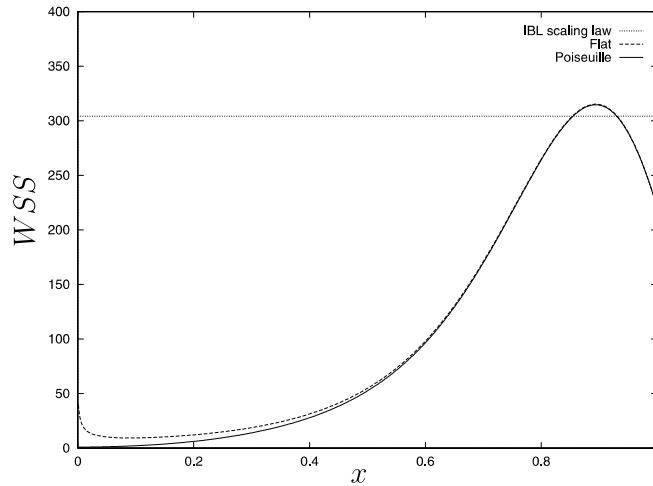


Fig. 16. Longitudinal evolution of the WSS along the convergent part of a 70% stenosis computed using the RNSP approach with $Re = 500$; solid line: Poiseuille entry profile; broken line: flat entry profile.

4. Conclusion

Having in mind applications in biomechanics, where the elevated wall shear stresses encountered in arterial stenoses are likely to play a role in the mechanisms of thrombo-embolism and atherosclerotic plaques ruptures, the purpose of this study is to evaluate the scale of the wall shear stress τ^* in a constricted pipe. Of course, the computation of such flows is now accurately achieved through Navier–Stokes solvers in a reasonable range of Reynolds numbers. On the other hand, simplified 1D theories and correlations from experimental data are available. Our work fills the gap between them. We claim that the asymptotic equations provide a better understanding of flow structure and of the relevant scalings as well. As computational time is reduced, parameters may be easily changed and their influence can be analysed. Thus, in this paper, we have presented a system that we call RNSP, referring to the Reduced Navier–Stokes equations, which are in fact the Prandtl equations with different boundary conditions. We have shown how to obtain the RNSP system from the NS system. Then, we have established the connection between the RNSP system and many other asymptotic descriptions of the Navier–Stokes equations, as summarised on Figs. 17, 18, and Table 1:

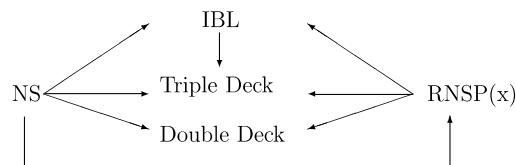


Fig. 17. The different models: RNSP is obtained from Navier–Stokes (NS). triple deck, double deck and IBL are obtained from NS, they may be obtained from RNSP in the pipe flow considered.

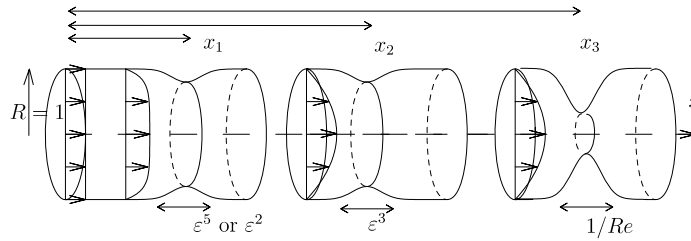


Fig. 18. Flow configurations: A constriction may be located at $x_1 = O(\epsilon^2)$ where an inviscid fluid core still exists; if the width is ϵ^2 IBL applies (Section 3.2.1). If the width is ϵ^2 the triple deck applies (Section 3.3). A constriction may be located at $x_2 > 1$ where the Poiseuille profile has developed, but the width has to be ϵ^3 for double deck (Section 3.4). If the constriction is short, but severe enough, IBL applies (Section 3.6.1).

Table 1

The scales may be tabulated in the following table (longitudinal length are scaled with $R_0^* Re$, transverse are scaled by R_0^*)

Model	RNSP	IBL	IBL	Triple deck	Double deck
Section	Section 2.2	Section 3.2.1	Section 3.6.1	Section 3.3	Section 3.4
Initial prof.	Any	Blasius	Any	Blasius	Poiseuille
Bump pos.	$x = O(1)$	$x = O(\epsilon^2)$	any	$x = O(\epsilon^2)$	$x > 1$
Bump width	Any	ϵ^2	$O(1/Re)$	ϵ^5	ϵ^3
Bump height	Any	ϵ	$O(1)$	ϵ^2	ϵ
Validity	$Re \gg 1$	$Re^{-1/2} \ll \epsilon \ll 1$	$Re \gg 1$	$Re^{-1/5} \ll \epsilon \ll 1$	$Re^{-1/2} \ll \epsilon \ll 1$

- First, the IBL equations deduced from the RNSP have been discussed. The entry effect has been computed using both the RNSP equations and a simple integral IBL description. They show a good agreement.
- We compared a full IBL resolution to a triple deck solution in the case of a very small constriction, located in the vicinity of a fully potential entry. The constriction height that promotes incipient separation was calculated using both triple deck theory and the IBL description.
- Then, the RNSP equations was compared with the double deck equations in the case of a small reduction of the pipe radius, assuming a fully viscous entry. The constriction height that promotes incipient separation was calculated using both the double deck theory and the RNSP description.
- A case of extremely long bumps leading to a Poiseuille flow was presented.
- Finally, a case where the initial potential flow is destroyed, leading to an IBL flow, has been studied. Maximum skin friction was calculated using simple IBL arguments. This permitted us to obtain an universal scaling law for the WSS.

A selected number of examples have been presented. Note that the gain in computational time is significant when compared with a full NS solution. Dimensional scaling allows a better understanding of various physical phenomena. In each section, the limits of the asymptotic descriptions was presented. The most interesting conclusion is that the transverse pressure gradient is irrelevant in a large number of cases. Thus, the flow in a constricted pipe is mainly ‘‘parabolic’’: the

disturbances propagate downstream and weakly upstream which allows marching computation (see [13] for a comparison between RNSP/IBL and full NS in case of reverse flow in a bidimensional configuration). In addition, the independence of the flow on the entry velocity profile has great implications because the in vivo entry profile is unknown and not parabolic as assumed in most studies.

In conclusion, it has been verified asymptotically and numerically that, in the pipe case, the RNSP(x) system agrees with most of the double/triple deck sets of equations and the IBL as well. Thus, the RNSP system may be used in cases of stenotic pipes. The bidimensional extension is straightforward. Extension to unsteady and non-axisymmetrical flows is currently in progress.

References

- [1] S.A. Berger, L.-D. Jou, Flows in stenotic vessels, *Ann. Rev. Fluid Mech.* 32 (2000) 347–382.
- [2] R. Budwig, D. Elger, H. Hooper, J. Slippy, Steady flow in abdominal aortic aneurysm models, *J. Biomech. Eng.* 115 (nov.) (1998) 419–423.
- [3] D. Bluestein, L. Niu, R.T. Schoepfoerster, M.K. Dewanjee, Steady flow in an aneurysm model: correlation between fluid dynamics and blood platelet deposition, *J. Biomech. Eng.* 118 (aug.) (1996) 280–286.
- [4] T. Cebeci, J. Cousteix, *Modeling and Computation of Boundary Layer Flows*, Springer-Verlag, 1999.
- [5] R.T. Davis, M. Barnet, J.V. Rakich, The calculation of supersonic viscous flows using the parabolized Navier–Stokes equations, *Comput. Fluids* 14 (3) (1986) 197–224.
- [6] B. de Bruin, P.-Y. Lagrée, S. Lorthois, C. Vilain, A.E.P. Veldman, Comparison of Navier–Stokes and reduced Navier–Stokes unsteady computation in a stenosis, *Arch. Physiol. Biochem.* 109 (09/2001) (2001) 79.
- [7] C.A.J. Fletcher, *Computational techniques for fluid dynamics. Vol. 2: Specific Techniques For Different Flow Categories*, Springer Series in Computational Physics, Springer-Verlag, 1988.
- [8] J. Gajjar, F.T. Smith, On hypersonic self induced separation, hydraulic jumps and boundary layer with algebraic growth, *Mathematika* 30 (1983) 77–93.
- [9] K. Gersten, H. Hervig, *Strömungsmechanik: Grundlagen Der Impuls-Wärme-und Stoffübertragung Aus Asymptotischer Sicht*, Vieweg, Wiesbaden, 1992.
- [10] H. Huang, V.J. Modi, B.R. Seymour, Fluid mechanics of stenosed arteries, *Int. J. Eng. Sci.* 33 (1995) 815–828.
- [11] P.-Y. Lagrée, Écoulement dans un anévrisme: comparaison de différentes méthodes de type couche limite, *Arch. Physiol. Biochem.* 106 (Supp B) (1998) 42.
- [12] P.-Y. Lagrée, An inverse technique to deduce the elasticity of a large artery, *Eur. Phys. J. Appl. Phys.* 9 (2000) 153–163.
- [13] P.-Y. Lagrée, E. Berger, M. Deverge, C. Vilain, A. Hirschberg, Characterization of the pressure drop in a 2D symmetrical pipe: some asymptotical, numerical and experimental comparisons, *ZAMM: Z. Angew. Math. Mech.* 85 (2) 141–146.
- [14] S. Lorthois, P.-Y. Lagrée, Écoulement dans un convergent axisymétrique: Calcul de la contrainte de cisaillement pariétal maximale/flow in a axisymmetric convergent: Evaluation of maximum wall shear stress, *C.R. Acad. Sci. Paris t328 Série II b* (2000) 33–40.
- [15] S. Lorthois, P.-Y. Lagrée, J.-P. Marc-Vergnes, F. Cassot, Maximal wall shear stress in arterial stenoses: Application to the internal carotid arteries, *J. Biomech. Eng.* 122 (6) (2000) 661–666.
- [16] J.C. Le Balleur, Couplage visqueux non-visqueux: Méthode numérique et applications aux écoulements bidimensionnels transsoniques et supersoniques, *La recherche Aérospatiale* 2 (1978) 67–76, *Eng Trans ESA TT-496*.
- [17] A.A. Maslov, S.G. Mironov, T.V. Poplavskaya, A.N. Shipliyuk, V.N. Vetlutsky, Viscous shock layer on a plate in hypersonic flow, *Eur. J. Mech. B/Fluids* 18 (2) (1999) 213–226.
- [18] T.J. Pedley, *The Fluid Mechanics of Large Blood Vessels*, Cambridge University press, 1980.
- [19] R. Peyret, T.D. Taylor, *Computational Fluid Dynamic*, Springer-Verlag, 1983.

- [20] T.A. Reyhner, F. Lotz, The interaction of a shockwave with a laminar boundary layer, *Int. Non-Linear Mech.* 3 (1968) 173–199.
- [21] A.I. Ruban, S.N. Timoshin, Propagation of perturbations in the boundary layer on the walls of a flat channel, *MZG* 2 (1986) 74–79.
- [22] S.G. Rubin, A. Himansu, Convergence properties of high Reynolds number separated flow calculations, *Int. J. Num. Meth. Fluids* 9 (1989) 1395–1411.
- [23] S. Saintlos, J. Mauss, Asymptotic modelling for separating boundary layers in a channel, *Int. J. Eng. Sci.* 34 (2) (1996) 201–211.
- [24] H. Schlichting, *Boundary Layer Theory*, seventh ed., Mc Graw Hill, 1987.
- [25] J.M. Siegel, C.P. Markou, D.N. Ku, S.R. Hanson, A scaling law for wall shear stress through an arterial stenosis, *ASME J. Biomech. Eng.* 116 (1994) 446–451.
- [26] F.T. Smith, Flow through constricted or dilated pipes and channels part 1 and 2, *Q.J. Mech. Appl. Math.* 29 (1976) 343–364, 365–376.
- [27] F.T. Smith, On the high Reynolds number theory of laminar flows, *IMA J. Appl. Math.* 28 (1982) 207–281.
- [28] K. Stewartson, Multistructured boundary layer on flat plates and related bodies, *Adv. Appl. Mech.* 14 (1974) 145–239.
- [29] J.S. Stroud, S.A. Berger, D. Saloner, Influence of stenosis morphology on flow through severely stenotic vessels: implications for plaque rupture, *J. Biomech.* 33 (2000) 443–455.
- [30] V.V. Sychev, A.I. Ruban, V.V. Sychev, G.L. Korolev, *Asymptotic Theory of Separated Flows*, Cambridge University Press, 1998.
- [31] J.C. Tannehill, D.A. Anderson, R.H. Pletcher, *Computational Fluid Mechanics and Heat Transfer*, second ed., Taylor & Francis, Washington, DC, 1997.
- [32] M. Van Dyke, *Perturbation Methods in Fluid Mechanics*, Parabolic Press, 1975.